

PART III

HR DIAGRAMS, SUBLUMINOUS STARS



Reception at the U.S. Naval Observatory, November 2, 1977.

THE HR DIAGRAM

Jesse L. Greenstein

Hale Observatories,
California Institute of Technology,
Carnegie Institution of Washington

The HR diagram is a useful shorthand locating a star in a two-coordinate space. For the astrophysicist, the y-coordinate is bolometric luminosity, M_{bol} , the x-coordinate, effective temperature, T_{eff} . Objects of given chemical composition, age (or evolutionary status) are labeled in the xy plane by mass. For an observer, y may be apparent or absolute magnitude in a certain wavelength region and x may be spectral type or color. The HR diagrams for populations differ because of age, chemical composition and stellar masses present. HR diagrams are often of mixed nature; some involve observables others derived or semi-theoretical quantities. I will display various types of HR diagrams for low-luminosity stars. For galactic or extragalactic studies the HR diagram needs a further dimension, the frequency of stars at an x,y. The mass of the Galaxy, but not its light, may be dominated by M dwarfs. HR diagrams are also interesting for their nearly empty spaces. In Fig. 1 we show as a sample, the basic results of the U.S. Naval Observatory parallax program, in which broad band (B-V) colors define the visual luminosity, M_V , on the main (MS) and degenerate (WD) sequences.

1. G-M STARS WITH THE MCSP

I report on work in progress on G-K-M dwarfs, stars of known parallax observed with the multichannel spectrophotometer (MCSP). I have observed 400 other proper-motion stars; parallax stars then calibrate photometric luminosities, $M_{1.85}$, tangential motions, T, and space motions, U,V,W. One program completed included all northern Lowell Observatory stars brighter than 16.5^m with motions

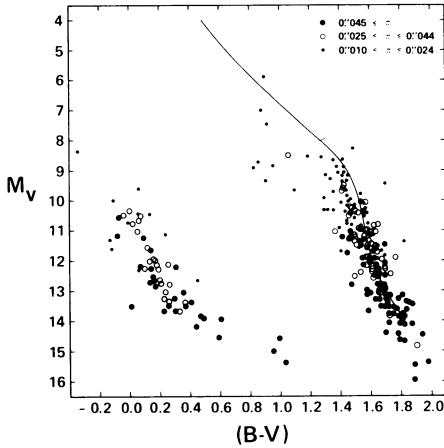


Fig. 1. The 330 USNO parallax stars, from Dahn *et al.* (1976) (their Fig. 2); symbols indicate size of parallax. Degenerate and main-sequence stars are well separated; (B-V) has only small amplitude for dM stars.

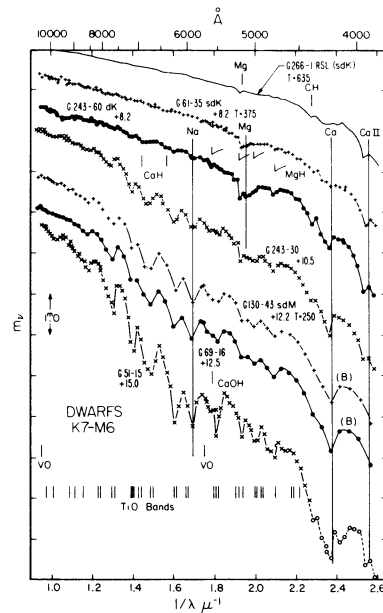


Fig. 2. MCSP output for a sample of main sequence stars; luminosities, $M_{1.85}$, and tangential motions, if high, are shown. The two curves labeled B are at lower resolution (80/160 Å). At the top is a "red subluminoous star", i.e., a weak-lined K star of unknown parallax; its color gives an extreme space motion.

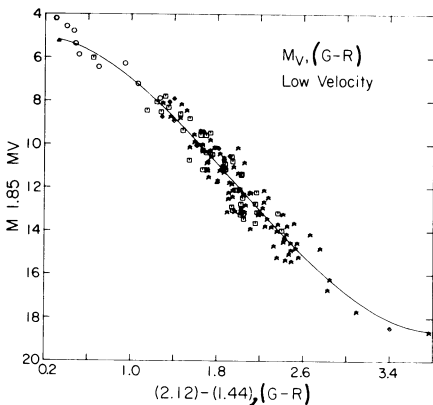


Fig. 3. Main-sequence stars of known parallax with $T < 100 \text{ km s}^{-1}$, showing MCSP color, (G-R), $[2.12] - [1.44]$ and $M_{1.85}$. Note the difference of shape of the lower main sequence from that in Fig. 1; symbols in Table I.

exceeding $1'0 \text{ yr}^{-1}$ (Giclas, Burnham and Thomas 1971). An additional 50 fainter stars (to $21^m.5$) from the Luyten Palomar Schmidt Survey (1969, 1970, 1974, 1976) have been observed. About one-third are degenerate; stars were selected either for "bluish" color or large reduced proper motion. The true numbers are distorted, weighted towards high-velocity stars; this is more than compensated by the rarity of high velocity among parallax stars.

The MCSP provides magnitudes or fluxes from 11500 to 3100 \AA . The accuracy, $\approx \pm 0^m.03$ is less than broadband, far less than Strömgren photometry. However, 31 photomultipliers observe a star simultaneously, with sky subtraction, so that colors are well determined. Depending on brightness, the resolution used is from 40 to 160 \AA ($\lambda < 5700 \text{ \AA}$) and 80 to 360 \AA ($\lambda > 5700 \text{ \AA}$). At highest resolution 155 data points are machine plotted; typical MCSP outputs are traced in Fig. 2. The information is too large to present in tabular form; for our purposes, monochromatic magnitudes, at frequencies in inverse microns, m_ν , are measured at 9 points. Magnitudes m_ν are represented by brackets or letters: $I^*=[1.00]$; $I=[1.25]$; $R=[1.44]$; $R^*=[1.52]$; $G=[2.12]$; $B=[2.35]$; $U=[2.80]$. The central frequencies used are related to some photoelectric systems, i.e., [1.85] is near the broadband V magnitude, at a less-absorbed position in dM stars. From O to K type stars, broad band $V=[1.85]-0^m.04$; $(B-V)=[2.35]-[1.85]+0^m.14$; $(U-B)\approx 0.97 \times ([2.80]-[2.35])-0^m.86$; $(R-I)_{\text{Kron}}\approx 1.11 \times ([1.44]-[1.25])+0^m.11$. These relations cannot be used in dM; the (R-I) relation is non-linear when $(R-I)_{\text{Kron}}$ exceeds $0^m.3$. The MCSP points were chosen by additional criteria, e.g., the strength of Ca I and TiO bands, sensitivity or freedom from TiO bands, strength of Mg I + MgH, [1.94], and Ca II + hydrogen, [2.58], not here discussed. Various color-luminosity diagrams can be derived from MCSP data.

The basic improvement in available parallaxes for faint stars was made with the new parallax reflector of the U. S. Naval Observatory at Flagstaff, constructed under the leadership of Strand (1971). Four papers with accurate parallaxes and UBV photometry have been published (Riddle *et al.* 1970; Routly 1972; Harrington *et al.* 1975; Dahn *et al.* 1976). These are among the first parallaxes with external errors only a small multiple of internal errors. Their small parallaxes can be used with some confidence, subject to an increase in the error of $\Delta M \approx 2.17 \Delta p/p$. At $\sigma \approx 0^m.003$ and $p = 0^m.019$ (a limit I have used) $\Delta M \approx 0^m.34$; even at 2σ , $\Delta M \approx 0^m.69$. Other recent parallax series from Lick (Klemola *et al.* 1975) and Yerkes (van Altena 1971, 1973a,b, 1975) are included, with weighted inputs. Old parallaxes have been included only if large and of high weight. The color-magnitude diagrams here presented are based on 237 G-M stars of parallax quality class 1-4. Table I shows the quality classes for the

TABLE I
QUALITY CLASSES AND SYMBOLS IN FIGURES

Q	$10^3 p$	Plot Symbol	
		T < 150	T ≥ 150
1	67	Star	*
2	40-67	Square	⊠
3	20-39	Diamond	X
4	10-19	Triangle	crosses

parallaxes and the symbols used in the diagrams. Old parallaxes have Q increased by unity, unless $> 0''.125$; the distribution of Q is Q = 1, 53%; Q = 2, 34%; Q = 3, 11% and Q = 4, 2%. Fits to the color-magnitude diagrams were made separately for a sample including objects, Q = 1,2, and those Q = 3 with several determinations. As discussed below, for high-velocity stars, solutions were obtained including Q = 3,4 stars, and separately for Q = 1,2 only.

Computer handling is necessary for such a mass of data. It introduces problems for individual objects such as unresolved binaries, suspected spectroscopic binaries, flare stars and objects with lower-quality MCSP. Some binaries ($> 6''$ separation) were resolved; unresolved pairs for which observers give $\Delta m \approx 0$ were corrected for duplicity. Unequal pairs, however, are difficult to handle and are treated as single. Some of the dispersion is caused by uncorrected duplicity (up to 0.75^m error); if the true error of a parallax can reach 2σ ($0''.006$ for USNO) at Q = 2, the dispersion introduced by the parallax is 0.33^m . Emission line and flare stars have errors in brightness and color, e.g., visible or ultraviolet emission during mini-flares, affecting B; H α is located in the R* band (6579 \AA). Observations at different resolutions have been used, with little effect in G, early K and degenerate stars, but with important effects in the later dm's. These are so faint at $v > 1.9 \mu^{-1}$, that we are forced to lowest resolution, ($160/360 \text{ \AA}$), and lower accuracy.

2. HR DIAGRAMS FOR PARALLAX STARS

The present data for 237 stars were computer processed to produce the diagrams separately for stars of high and low tangential velocities. Selection prevents the parallax and proper-

motion-magnitude-limited samples from containing many halo stars. If halo stars of a given M are 10^{-3} as common as old disk and Population I, the nearest example is 10 times further and 5^m fainter. Since sdM distances are small the z -direction density gradient may be neglected. I had initially planned two samples separated at $T > 150 \text{ km s}^{-1}$, to select halo stars. The symbols are, in fact, so divided; but only 12 stars have $T > 150 \text{ km s}^{-1}$, ($Q = 1,2$); $Q = 3,4$ makes the total 58. Only 46 stars with $Q = 1,2$ have $T > 100 \text{ km s}^{-1}$.

HR diagrams are shown (Figs. 4-6) for $T < 100 \text{ km s}^{-1}$, $Q = 1,2$. The fitted cubic, and dispersions, prove MCSP colors useful for calibration of stars of unknown parallax. In Fig. 7 are plotted $T > 100 \text{ km s}^{-1}$, $Q = 1,2$ stars individually; the cubic obtained on adding $Q = 3,4$ stars is shown.

Comparison of Figs. 1 and 5, shows that B colors on the MCSP, unlike the broadband, increase rapidly as luminosities decrease. No discontinuity exists in the MS slope. Use of infrared colors give smaller range in infrared M ; the large amplitude of the M_V diagram is caused by TiO and line blocking. The MS stars are clearly separated from the degenerates in Fig. 1, as they are in MCSP diagrams. In the MS broadband M_V , (B-V) diagram, +8 to +17, the slope is 13; in the $M_{2.35}$, [2.35]-[1.85] MCSP diagram the slope is 5.3. The $M_{1.85}$ is less than broadband M_V in dM stars, since [1.85] is at high flux (Fig. 2); the broadband V averages strong absorptions on a steep flux gradient. Bolometric corrections based on $M_{1.85}$ are smaller, and less composition-sensitive. The use of even broadband (R-I) will certainly improve the HR diagrams produced by the USNO program.

Details of the least-square fits will be published elsewhere. Dispersions about the cubics, σ , are about $0^m.53$ for $T < 100 \text{ km s}^{-1}$, $Q = 1,2$; the $M_{1.85}$, (G-R) and $M_{2.35}$, (B-V), have $\sigma = 0^m.72$. For the $T > 100$ group, $\sigma \approx 0^m.57$; inclusion of $Q = 3,4$ gives $\sigma \approx 0^m.70$. Part of the scatter arises from uncorrected duplicity, flare stars (which cause bad scatter in the (B-V) diagram) and poor photometry in the blue-violet, where late dM stars reach 22^m , but much arises from parallax errors.

Among 179 good stars, 23 have relatively reliable $Q = 3$ parallaxes; 58 more with $Q = 3,4$ exist, of which 39 have $T > 200 \text{ km s}^{-1}$, a few $T > 500 \text{ km s}^{-1}$. Inclusion of $Q = 3,4$ gives a more genuine high-velocity sample, at the cost of larger $\Delta p/p$, and σ increases 25%. The general result is that high-velocity stars, $Q = 1,2$, are fainter by $\Delta M_{1.85} + 6^m < M_{1.85} < +10^m$. $\Delta M_{1.85}$ disappears, generally, by $+11^m.5$, and possibly forced by the cubic fit, $\Delta M_{1.85} \approx -0^m.3$ for the faintest stars. Including $Q = 3,4$, a purer high-velocity sample, increases $\Delta M_{1.85}$ to reach 14^m ,

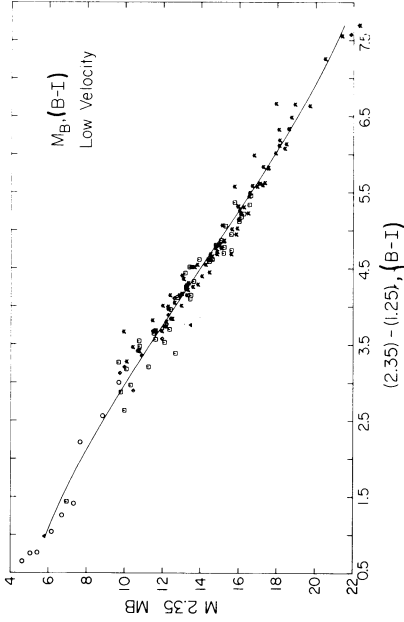


Fig. 5. Blue HR diagram, lower accuracy.

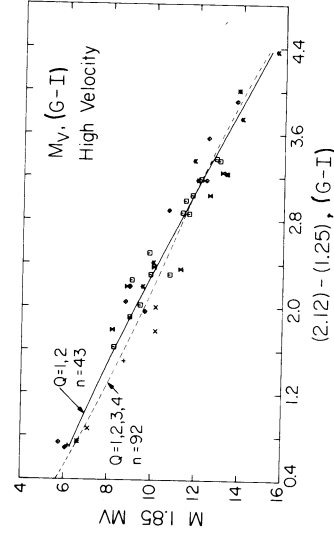


Fig. 7. Individual high-velocity stars, $Q = 1, 2$. Lower quality solution dashed.

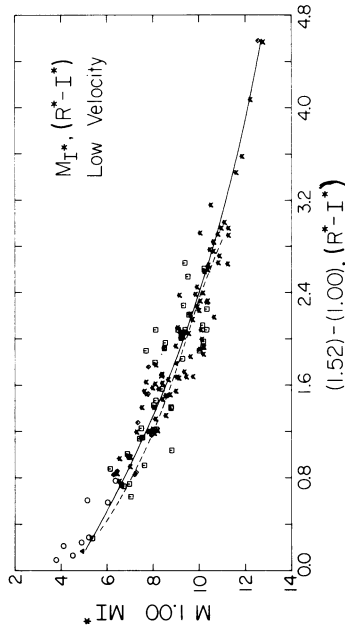


Fig. 4. HR diagram for a band-free color. $M_{1.00}$ is close to M_{bol} . High-velocity cubic dashed.

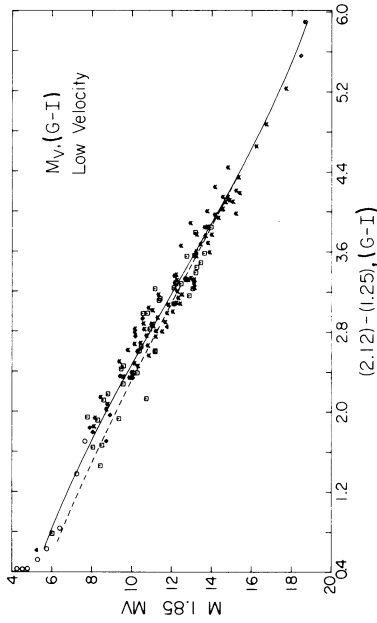


Fig. 6. (G-I) diagram, $\sigma = 0.051$; high velocity dashed.

probably to $M_{1.85} = +12^m$. HV stars are subluminous in all MSCF colors, therefore.

Nine Hyades stars are shown in the figures as open circles; but are not used in the fitting. Eggen (1973, 74 and elsewhere) used broadband (R-I) to separate old disk from young stars (e.g., the Hyades), and from the true halo population. He suggests that the Hyades contains stars above the ZAMS evolving to the MS, and brighter stars evolving upwards. The Hyades and the $M_{1.25}$ [1.44 - 1.25] results are shown in Figs. 4-6 and in Fig. 8. Four are 0^m1 bluer than the program stars, and are 0^m7 above the extrapolated, nearly straight-line, least-squares fit. Those with $m_y(R-I) > +0^m12$ deviate by less than 0^m1 .

A systematic error arises from the selection of parallax stars to observe, since stars of negative or small parallax are not included. The sample including poorer p ($Q = 3,4$) has $\langle p \rangle = 0^m135$ for $T < 100 \text{ km s}^{-1}$, 0^m074 for $100 < T < 200 \text{ km s}^{-1}$ and only 0^m032 for $T \geq 200 \text{ km s}^{-1}$. The asymmetrical nature of the error can be estimated. For the larger parallaxes with $\sigma = \pm 0^m003$, $\pm 1\sigma$ produces errors in M of -0^m23 and 0^m20 ; for $\pm 2\sigma$ the errors are -0^m49 and $+0^m39$; for $\pm 3\sigma$, -0^m78 and 0^m57 . Selected by apparent, not true parallax, stars suffer a systematic dimming by $+0^m02$, $+0^m05$ and $+0^m10$. Repeating the exercise at $\langle p \rangle = 0^m20$, however, gives $\langle \Delta M \rangle = +0^m03$, $+0^m11$ and $+0^m25$, and at $\langle p \rangle = 0^m015$, $\langle \Delta M \rangle = +0^m04$, $+0^m19$ and $+0^m49$. This effect is negligible at 1σ , nearly so at 2σ , but is comparable to the population-type luminosity difference ΔM , at 3σ . The USNO observers have not underestimated their external error by 3, nor do recent Lick and Yerkes parallaxes have errors approaching $\pm 0^m010$. They agree well with USNO values where they overlap. Thus, we have established the degree to which high-velocity stars are subluminous, found it to disappear by mid dM, and to be independent of color baseline; i.e. it is probably not caused by line and band blocking.

Unexpectedly the high-velocity stars appear most subluminous (by at least 0^m6) at the bluest colors at which they exist in my sample (early G). If metal-poor late-type stars exist, differential line blocking makes them bluer. In banded stars, TiO would vary as the square of the metal abundances; Population II early sdM stars are, in fact, recognizable by strong MgH and CaH compared to TiO. The colors here used are as insensitive to line blocking in the red for sdG and early sdK stars, as for dG and dK stars. Yet (G-R), (R*-I*) and (R-I) agree in making our bluest "high-velocity" stars 0^m6 fainter than stars of corresponding color. The $\langle T \rangle = 149 \text{ km s}^{-1}$ for the high-velocity stars, and $\sigma = 75 \text{ km s}^{-1}$, i.e., does not give a truly Population II sample. The parallax sample is dominantly old-disk population, with some low-velocity Population I stars present. The F to K Hyades stars may be

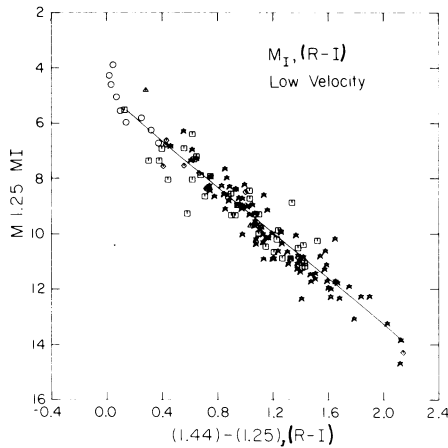


Fig. 8. The $M_I, (R-I)$ diagram for low-velocity stars is nearly linear. The four bluest Hyades stars measured (open circles) may lie above the relation extrapolated from parallax stars, but, the few redder Hyades fit well.

brighter than old disk stars; the "high-velocity" stars, $T > 100 \text{ km s}^{-1}$, are appreciably fainter at the blue color where evolution removes them from the Population II main sequence. It is particularly surprising that they are faintest there, rather than brighter, i.e., subgiants.

3. THE HIGH-VELOCITY POPULATION

A fundamental difference between the $T \leq 100 \text{ km s}^{-1}$ diagrams is that the higher-velocity group lacks intrinsically faint and very red stars. In part this is a selection effect, but my continued search among fainter, redder stars with no available parallax suggests that high-velocity stars continue to be rare. The faintest low-velocity stars are $M_{1.85} = +18^m.8$ (LP619-50, Van Biesbroeck 10), near $M_{2.35} = +22^m.0$. The faintest stars with $T \approx 200 \text{ km s}^{-1}$, G34-15, G260-1 (LP71-157), have $M_{1.85} = +13^m.2$, $M_{2.35} = +16^m.2$. Only seven stars have $M_{1.85} > 12^m.0$, and $T > 200 \text{ km s}^{-1}$. Parallaxes for apparently fainter stars of large proper motion are clearly badly needed. I have already observed about fifty red stars from the LP and LHS catalogs using the MCSP; using the present calibration I will estimate luminosity, parallax and space motion. These stars, of course, are faint, 17^m to 19^m visual, and will be difficult objects for any parallax telescope. A few stars as red as LP619-50 and VB 10 have already been found, but none so far redder. In my catalog (July 1977) of

465 space motions a problem in the search for high-velocity late-type stars became apparent. I studied the photometric luminosity of 81 stars which lack parallax and have $T \geq 250 \text{ km s}^{-1}$. The median $M_{1.85} = +7.5$; only five stars have $M_{1.85} > +10.0$ and the faintest is $+11.2$. The Lowell proper-motion stars are limited to 16^m5 photographic; intrinsically faint sdM stars will be found only by systematic colorimetry beyond 20^m, photographic.

One example of the interesting ultra-high-velocity, so-called RSL stars has been shown in Fig. 2, G266-1 (LHS 4037) an extremely weak-lined, yellow sdK. The mean of four MCSP scans gives $M_{1.85} = +7.2$. From its proper motion and radial velocity $T = 635 \text{ km s}^{-1}$, and the space motion is $U = +223$, $V = -606$, $W = -2 \text{ km s}^{-1}$. The star is metal-poor and not degenerate. Photographic and SIT spectra at 3 Å resolution show sharp Ca II, Ca I, Mg I, extraordinarily strong CH, and ultraviolet Fe I. Can differential line blanketing falsify the photometric luminosity? The six different colors used predict, however, a parallax of 0.0055 ± 0.0002 , so consistent that differential line blanketing cannot be important.

Such stars had been noted earlier by Eggen (1969); Greenstein had called them "Eggenites" (1969); more recently they have been called RSL (red subluminous). They exist in considerable numbers; none has a recently measured parallax. Their true location in the HR diagram is unknown. If extremely metal deficient, they may lie in a color-color diagram on the locus between normal-metal dM's and an unblanketed dM star, or one with blanketing included theoretically (Greenstein 1969; Tsuji 1969). Very metal-poor sdM's might be confused with sdK's, and late sdM's with earlier subtypes. Lack of recognition of this could increase the numbers of low-luminosity halo stars, but it would also decrease their deduced tangential velocities. Such stars may be genuinely subluminous as compared to our presently defined high-velocity group of parallax stars, but whether by $\Delta M \approx +1^m$ or $+3^m$ is not yet known. With the latter value, they could have measurable parallaxes.

4. SPECTRAL TYPES

The complex spectra and faintness of dM stars resulted in published spectral classifications being on inconsistent scales. An accurate classification is given by Boeshaar (1977) from estimated relative strengths of the bands TiO, VO, CaOH in the visual region. Color-spectral-type relations are shown in Fig. 9 for stars in common, using $(R^* - I^*)$, i.e., not that of a truly Population II sample. The narrower baseline (R-I), more strongly affected by TiO, has a 1^m3 amplitude.

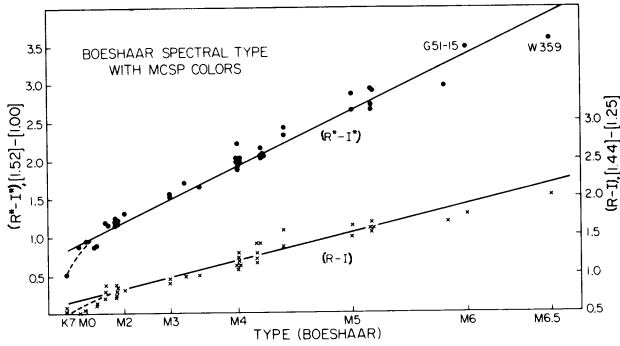


Fig. 9. Color-spectral type (P. Boeshaar's thesis). Types are on an exponential scale.

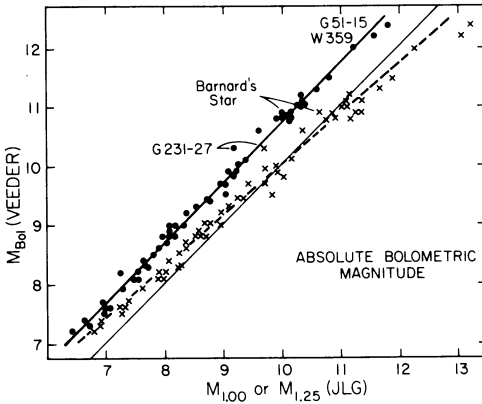


Fig. 10. Veeder's M_{bol} compared with MCSP absolute magnitudes, same parallaxes. Scatter among the faintest stars is partly observational error. A halo star deviates appreciably to the left.

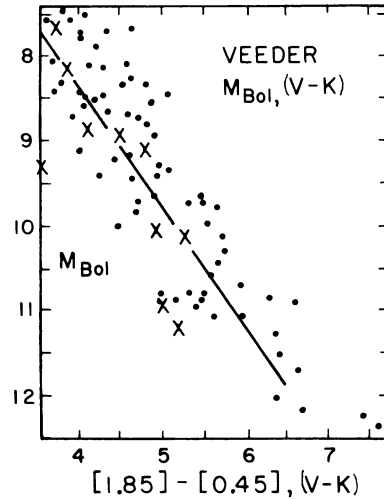


Fig. 11. Veeder's bolometric magnitudes and infrared visual color. X = halo stars.

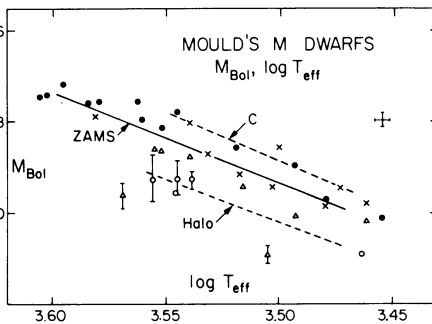


Fig. 12. M_{bol} and T_{eff} from Mould and Hyland. The upper dashed line (C) is for possible contracting stars, the lower for the halo. Filled circles, old disk; open circles & crosses halo. Kapteyn's star is the open circle at 9.53^m , $\log T_{eff} = 3.546$.

Both relations, shown in Fig. 9, are approximately linear later than M1. Note, however, that spectral type had to be plotted on a logarithmic scale! Colors transform to spectral type, with an accuracy better than 0.5 subtype. Boeshaar has shown that a significant, precise spectral type can be determined in the red and near infrared which is well correlated with luminosity.

5. BOLOMETRIC MAGNITUDE DIAGRAMS

Consider the theoretical HR diagram giving absolute bolometric magnitude, M_{bol} , as a function of blanketed infrared colors, or, best of all, of effective temperature. Such diagrams are still remote goals but progress has been made. Infrared measurements in broadband J, K, L, M by Johnson (1965) first gave a T_{eff} scale; Greenstein, Neugebauer and Becklin (1970) redetermined lower-main-sequence radii, T_{eff} , and bolometric corrections. Veeder (1974) measured infrared colors of a number of dM stars with $p > 0.100$. Extrapolation from broadband infrared colors to total flux is not difficult, Veeder having used a blackbody fit. His M_{bol} were available for 58 stars with MCSP data; after minor readjustment in parallaxes used we compare Veeder's M_{bol} with our near-infrared $M_{1.00}$ and $M_{1.25}$. In Fig. 10 we show how good these relations are; they seem independent of space motions or the presence of emission. The linear relations fitted are:

$$M_{bol} = 1.014 M_{1.00} + 0.460,$$

$$M_{bol} = 0.863 M_{1.25} + 1.41.$$

In dM stars, $M_{1.00}$ differs from M_{bol} only by a constant; $M_{1.25}$ has a 15% difference in scale.

Individual stars are shown in Fig. 10, as well as the linear relations. The M_{bol} , $M_{1.25}$ relation is significantly non-linear. The faintest, reddest stars deviate to the right suggesting that measures of I^* are depressed by TiO bands near 1μ . Barnard's star is slightly to the left of the mean relations; although called subluminoous, it is not very high velocity, $U = -141 \text{ km s}^{-1}$. If subluminoous it is by nearly the same amount at [1.00], [1.25] as bolometrically. One star (observed twice), G231-27, shifts much further to the left. It has strong hydride bands, a halo space motion (+372, -196, -117 km s^{-1}), and the photometric $M_{1.85}$ from different baselines are accordant. For an unknown reason it is depressed at $\lambda > 9000 \text{ \AA}$, as if an additional source of band absorption existed (CN and FeH are candidates). With few exceptions, dM stars are so remarkably homogeneous that we must ask: Where are the extremely metal-poor stars?

Veeder (1974) gives an HR diagram using infrared K ($2.0 - 2.4 \mu$) at $v = 0.45 \mu^{-1}$, yielding M_{bol} , (V-K) as reproduced in Fig. 11.

The straight line is: $M_{\text{bol}} = 1.12 M_{0.45} + 1.181$. As expected, the scale factor is large for $M_{0.45}$. He believes cosmic scatter to be real. There is little difference between high- and low-velocity stars, although in a true L, T_{eff} diagram, metal-poor stars lie below the normal ZAMS. There should be little effect of band blocking on M_{bol} , or on K . Band blocking could appear as extra absorption at V , i.e., as shifts to the left.

Mould's (1976) thesis at the Australian National University attempts to produce a true $(M_{\text{bol}}, T_{\text{eff}})$ diagram. For Kapteyn's star, with halo motion, $V = -288 \text{ km s}^{-1}$, Mould and Hyland (1976) find a metal deficiency of a factor of 3 to 4, using blanketed model atmospheres. The star is 1.70 below the bolometric ZAMS at $T_{\text{eff}} = 3500 \text{ K}$. They have not as yet displayed a large intrinsic luminosity deficiency for sdM stars, as shown in Fig. 12. Our ΔM for sdG or sdK stars is apparently maintained in early M, although the abundance deficiencies at the surface seem smaller than at sdG.

6. THE DEGENERATE STARS

This subject deserves nearly as much attention as the MS; my MCSP work has been mostly presented in Greenstein (1976). Only a modest increase in the data (MCSP, or Strömgren photometry) has since occurred. Many new degenerates have been discovered at the Steward and Hale Observatories. Parallaxes are badly needed for the yellow and red degenerates at the bottom of the cooling sequence. Splitting degenerate stars of known parallax into high- and low-velocity groups is not yet feasible. The main problems are such questions as (1) What is the composition sensitivity of the HR diagram? (2) Do discrete cooling sequences exist? (3) What is the spread of masses among degenerate stars? Infrared measures have not been carried out for the red degenerates to give bolometric corrections; since lines and bands are weak, model atmospheres may be sufficient to obtain M_{bol} . The extreme ultraviolet measures from space, as well as the ANS satellite program in the nearer ultraviolet provide better effective temperatures for hot stars permitting construction of an $M_{\text{bol}}, T_{\text{eff}}$ diagram. Temperatures determined to be above 10^5 K mean that WD's exist from $10 L_{\odot}$ to well below $10^{-4} L_{\odot}$. Many red degenerates have been found as red and faint as any known in 1976, mostly among the Luyten Palomar survey. Most are DC metal-poor at the surface, except for LP701-29 (Dahn et al. 1977), by 0.6 the faintest known degenerate at $M_V = 16.1$. But LP542/3 is a double red degenerate found by van Altena, who is measuring its parallax; Palomar spectra show both to be DC, with $M_V = 15.6$ and 16.0 . Thus, large composition variations are found among the faintest degenerates, unlike MS stars. From this point of view, HR diagrams for the degenerate stars are instructive. The $M_V, (G-I)$ diagram from Greenstein (1976)

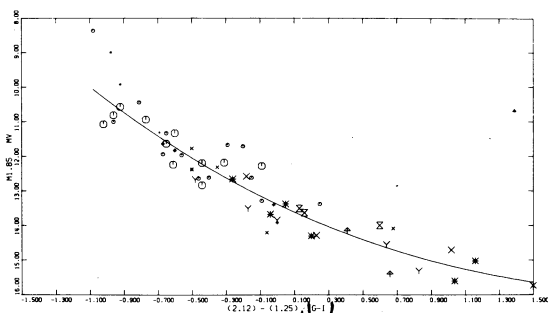


Fig. 13. M_V for degenerate stars as function of a color which is relatively composition insensitive, $\sigma = 0.56$.

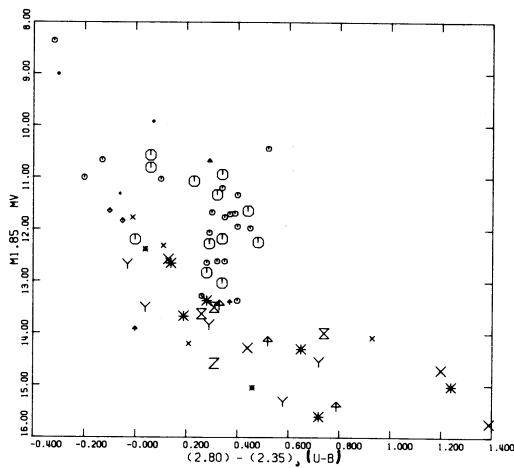


Fig. 14. M_V for WD's is poorly correlated with (U-B). The Balmer jump, absent in non-hydrogen stars, dominates and the scatter is large.

is shown in Fig. 13. The surface composition is probably irrelevant; only carbon degenerates have strong features in the MCSP [2.12] region. Only one star, EG 38 (upper right) is far off the mean curve; it is a composite, DA+dM. The symbols are: Octagons, hydrogen-rich; diamonds, helium-rich; stars, metals present; X, no lines. Compare the scatter with that in Fig. 14, where the color used is composition sensitive, i.e., it spans the Balmer jump. Colors of models for hydrogen atmospheres of increasing temperature run almost vertically at $(U-B) = 0.4$, to rejoin the sequence of helium dominated atmospheres near -0.2 . The recognition of degenerates of differing surface composition is best done in a color-color diagram. Residual vertical scatter in a suitable HR diagram, which could be bolometric, is either a spread in mass (i.e., radius), or an effect of composition on color. This work was supported in part by the NSF, AST77-09191.

REFERENCES

Boeshaar, P. C. (1977). The Spectral Classification of M-Dwarf

- Stars, preprint from unpublished Ph.D. thesis, Ohio State University.
- Dahn, C. C., Harrington, R. S., Riepe, B. Y., Christy, J. W., Guetter, H. H., Behall, A. L., Walker, R. L., Hewitt, A. V., and Ables, H. D. (1976). Publ. of the U.S. Naval Obs. 20, part 3, U. S. Government Printing Office, Washington.
- Dahn, C. C., Hintzen, P. M., Liebert, J. W., Stockman, H. S., and Spinrad, H. S. (1977). in press.
- Eggen, O. J. (1969). in Low Luminosity Stars, S. S. Kumar, ed., Gordon and Breach, New York, p. 3.
- _____. (1973). Astrophys. J. 182, 821.
- _____. (1974). Publ. Astron. Soc. Pacific 86, 697.
- Giclas, H. L., Burnham, R. Jr., Thomas, and Thomas, N. G. (1971). The G Numbered Stars, Lowell Obs., Flagstaff. Also Lowell Obs. Bulletins.
- Greenstein, J. L. (1969) in Low Luminosity Stars, S. S. Kumar, ed., Gordon and Breach, New York, p. 281.
- Greenstein, J.L. (1976). Astron. J. 81, 323.
- Greenstein, J. L., Neugebauer, G., and Becklin, E. E. (1970). Astrophys. J. 161, 519.
- Harrington, R. S., Dahn, C. C., Behall, A. L., Priser, J. B., Christy, J. W., Riepe, B. Y., Ables, H. D., Guetter, H. H., Hewitt, A. V., and Walker, R. L. (1975). Publ. of U. S. Naval Obs. 24, part 1, U. S. Government Printing Office, Washington.
- Johnson, H. L. (1965). Astrophys. J. 141, 170.
- Klemola, A. R., Harlan, E. A., McNamara, B., and Wirtanen, C. A. (1975). Astron. J. 80, 642.
- Luyten, W. J. (1969). Proper Motion Survey with the 48-inch Schmidt Telescope XIX, University of Minnesota, Minneapolis. Also others of this series.
- _____. (1970). White Dwarfs, University of Minnesota, Minneapolis.
- _____. (1974). Proc. Nat. Acad. Sci. 71, 4813.
- _____. (1976). Catalogue of Stars with Proper Motions Exceeding 0!5 Annually, University of Minnesota, Minneapolis.
- Mould, J. (1976). Ph.D. thesis, Australian National University, Canberra.
- _____. (1976). Astrophys. J. 210, 402.
- Mould, J., and Hyland, A. R. (1976). Astrophys. J. 208, 399.
- Riddle, R. K., Priser, J. B., Strand, K. Aa., and Riddle, R. K. (1970). Publ. of the U.S. Naval Obs. 20, part 3A-3C, U. S. Government Printing Office, Washington.
- Routly, P. M. (1972). Publ. of the U.S. Naval Obs. 20, part 6, U. S. Government Printing Office, Washington.
- Strand, K. Aa. (1971). Publ. of the U.S. Naval Obs. 20, part 1, U. S. Government Printing Office, Washington.
- Tsuji, T. (1969). in Low Luminosity Stars, S. S. Kumar, ed., Gordon and Breach, New York, p. 457.

- van Altena, W. F. (1971). Astron. J. 76, 932.
van Altena, W. F., and Vilkki, E. U. (1973a), Astron. J. 78, 201.
van Altena, W. F., and Stone, R. C. (1973b). Astron. J. 78, 781.
van Altena, W. F., and Vilkki, E. U. (1975). Astron. J. 80, 647.
Veeder, G. (1974). Astron. J. 79, 1056.

DISCUSSION

UPGREN: Did you correct the absolute magnitudes derived from parallaxes for the volume effect such as Lutz and Kelker have found?

GREENSTEIN: I am familiar with the correction, which Eddington first derived, and the Malmquist corrections and their effect on the mean luminosity. There exists an asymmetry, which depends on the ratio of the parallax to its true mean error. These are trivial except for the smallest parallaxes used. The evidence that high-velocity stars are subluminous by 0.76, on the average, would disappear only if the true errors of the USNO, new Yerkes, Lick parallaxes were, in fact, three times their quoted values, which I do not believe.